Saeed Baghernezhad[1], Mohammad Ghane[1], Meysam Moezzi[2]

Strain Monitoring in Woven Fabrics with Locally Induced Mass Irregularities Using an Image Based Method

DOI: 10.5604/12303666.1191430

[1)] **Department of Textile Engineering, Isfahan University of Technology,**
Isfahan, 84156-83111, Iran

[2)] **Department of Textile Engineering, Faculty of Engineering, University of Bonab,**
Bonab, 55517-61167, Iran
E-mail: meysammoezzi@bonabu.ac.ir

Abstract
The aim of this work was to study the effect of induced mass irregularities of yarn on the strain monitoring of fabric during a tensile test. Slub yarns with different induced mass irregularities were produced and used as weft yarns in plain woven fabric. The Digital Image Correlation (DIC) method was used to evaluate the strain distribution map of the fabric during the tensile test. Images of the reference sample as well as of the strained fabric under the sequential strain applied were captured. By applying the DIC method, a strain distribution map of the fabric at a certain value of the strain applied was calculated for all samples. Results of the strain map calculated were then compared with the image of the actual fabric. It was found that there was good agreement between the map of strain distribution calculated by DIC and the local concentration of strain in the fabric. The results also revealed that the variation in strain distribution in the fabric during the tensile test was correlated exponentially to the breaking stress in cN/tex) of yarn as well as the breaking strength in N of the fabric.

Key words: *full field strain monitoring, damage prediction, mass irregularities, slub yarn, digital image correlation.*

Introduction

Woven textiles consist of two perpendicular sets of yarns, i.e., warp and weft. The physical properties and characteristics of the constituent yarns dictate the properties and behaviour of the fabrics. Among the different properties of the yarn, mass irregularities can have a significant effect on the stress-strain properties of the fabric.

Different techniques have been employed to induce controlled local irregularities in the yarns, which are so called 'effect' yarns [1, 2]. One of the techniques commonly applied is the use of slub yarns. Simply defined, slub yarn contains a thick and thin place in its length. This yarn is one of fancy yarns with structural effect categories.

According to ***Figure 1***, slub yarns contain many structural parameters such as the slub length, slub distance, base yarn count and ramp section [3]. Slub yarns are often produced by a ring machine with a servomotor on its middle and back roller. This yarn can also be produced by an open-end machine. However, because of these limitations in the slub length and distance, in practice, this way is not commonly used. The length of slub patterns can vary from small to high.

Lu et al [4] developed a model considering the shearing modulus and the polar moment of inertia of the yarn. Applying analysis and solving the corresponding equations, they could attain twist distribution in the slub yarns. They found that the twist distribution of the slub yarn could be deduced through the bar torsion model. The experimental results also showed that the twists calculated were very close to the experimental results. They also concluded that the twist in every section of the slub yarn was inversely related to the square of the linear density of the corresponding section.

İlhan et al [5] developed a theoretical model used for calculating the average count of slub yarn. To investigate the usability of the model, they produced a yarn sample by ring machine and then the actual counts were investigated. As a result of the correlation analysis, they concluded that there was a very strong correlation ($R^2 = 0.984$) between the predicted and actual values.

İlhan et al [3] studied the effect of descriptive parameters of slub yarn on the strength and elongation properties using the full factorial design method. They stated that the most significant

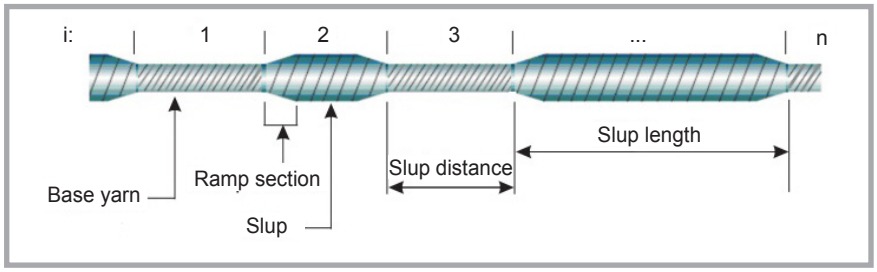

Figure 1. *Schematic mode of slub yarn [3].*

parameters affecting the breaking force of the slub yarn samples were the slub length, slub distance and the base yarn count. The parameters affecting the elongation at break of the slub yarn samples were found to be the slub multiplayer, base yarn count and twist coefficient.

Souid et al [6] attempted to develop a credible approach for determination of the quality of ring spun and slub yarns by virtue of criteria incorporating combinations of the fundamental fibre characteristics. They investigated the possibilities of using global optimization superimposed diagram response surface methodology in order to identify spinner feasibility conditions across customer yarn quality requirements.

Pan et al [7] described a new method for recognising the parameters of slub yarn based on image analysis. They wrapped slub yarn on the surface of a blackboard with a YG381 yarn evenness tester. A high-resolution scanner was used to acquire the yarn image and Gray stretching and thresholding were carried out to preprocess the image of slub yarn. They were able to find the periodicity rule and the period of slub yarn by listing the slub length and distance in a visualization plot. Histogram charts were obtained and then slub yarn parameters were determined.

In all mechanical deformation, including tensile deformation, the failure of the damage is initiated in the weakest part (zone) of the materials. In some engineered textiles, the analysing and prediction of the onset of failure or the damage zone is of great importance as it can be useful to identify the weakest points and make necessary measurements to enforce the textile structures.

In most researches, it is assumed that the fabric thickness is homogenous and uniform along and across the fabric. However, in practice, there are different sources of irregularities in the yarn and fabric, leading to un-uniformity in the fabric thickness. This unevenness causes each element of the fabric surface to behave differently during the tensile tests [8, 9].

Slub yarns are widely used for fabric production. Due to the nature of these yarns, the difference between the thick and thin places is very high, leading to high variation in the fabric thickness, which is very important in analysing the strain distribution in slub fabric during the tensile test.

Because of the different distribution in the strain field, during the deformation of a material, the damage in each element of the material surface can appear at a different level [10]. Full field strain monitoring can help to predict the damage in every element of the surface [11, 12]. Some researchers have suggested image processing based methods for strain characterisation of woven fabrics [13 - 15]. Thus we can select a digital image correlation to monitor the strain and damage in irregular and faulty surfaces [16].

Table 1. *Average results of slub yarn parameters.* ***Note:*** *The values in brackets represent percentage coefficients of variations.*

Samples	Slub part mean linear denacity, tex	Base part mean linear denacity, tex	Slub distance, cm	Slub length, cm	σ_{max} yarn, cN/tex
1	24.11 (9.16)	15.52 (5.12)	14.60 (8.50)	3.90 (7.12)	15.94 (10.64)
2	29.33 (9.21)	14.52 (3.41)	18.98 (8.57)	9.30 (5.21)	8.74 (12.49)
3	25.33 (9.50)	14.74 (8.60)	36.6 (10.86)	3.30 (6.78)	10.49 (12.23)
4	28.28 (4.50)	16.98 (6.60)	14.39 (5.36)	4.33 (4.34)	16.08 (11.89)
5	29.19 (12.40)	16.33 (2.40)	7.34 (7.82)	5.42 (8.93)	10.39 (10.24)
6	19.68 (2.66)		-		16.15 (11.04)

Table 2. *Results of fabric tensile properties.* ***Note****: The values in brackets represent percentage coefficients of variations.*

Fabric sample	Tensile strength (F_{max}), N	Elongation, mm	Work of rupture, Nmm
1	110.6 (4.47)	9.61 (10.72)	591.37 (2.94)
2	40.98 (2.69)	7.81 (10.34)	189.92 (8.84)
3	68.74 (6.76)	7.50 (13.09)	276.49 (10.55)
4	113.22 (4.59)	9.09 (10.87)	548.99 (6.43)
5	64.27 (7.06)	8.21 (13.35)	312.46 (10.87)
6	114.83 (7.39)	13.57 (13.38)	862.92 (4.7)

As a powerful and flexible tool for surface deformation measurement, digital image correlation (DIC) [17, 18] has been widely accepted and commonly used in the field of experimental mechanics. With the DIC technique, full-field displacements with sub-pixel accuracies [19, 20] and full-field strains can be directly computed through processing grayscale digital images of the specimen surface as recorded before and after deformation. More recently, the methodologies of the existing 2D DIC technique for displacement and strain measurements have been systematically reviewed in a review paper by Bing Pan [20].

Apart from the subset-based DIC method, it should be noted that some other techniques, for instance, the point wise DIC method based on the genetic algorithm developed by Jin and Bruck [21], the continuum DIC method based on the B-spline deformation function proposed by Cheng et al., [22] and the DIC method based on the finite element method presented and improved by Sun et al., [23]and Hild et al., [24 - 26], may be able to determine the displacement of each pixel within a selected region of interest (ROI). It is also well-known that the DIC technique based on the most widely used Newton-Raphson (NR) algorithm requires an accurate initial guess to converge rapidly and reliably [25, 26]. In the existing DIC technique, the deformation vector of the current point determined is used as the initial guess of the next point. This straightforward initial guess transfer scheme can be easily carried out for a simple rectangular ROI. However, for an irregular ROI defined for an object comprising geometric discontinuities, the initial guess transfer between the neighboring points can be challenging when ensuring reliable and accurate measurements is important [27].

The main aim of this study was to investigate the effect of locally induced irregularities of yarns or slub yarn parameters on the strain distribution of a fabric during a tensile test. To analyse the strain at each point of the fabric, the subset-based DIC was used. Moreover, by this method, we monitored the strain distribution and predicted the maximum points of strain that caused rupture in the fabric, as it was related to slub yarns and fabric specifications with high accuracy.

Materials and method

Slub yarn production

Five different kinds of slub yarns were produced by a Reiter ring spinning machine. These yarns were different from each other in terms of slub patterns. For comparison of these slub yarns and regular yarns, a sample of regular yarn was produced by a ring spinning machine.

All yarns, made from cotton, were produced at the same linear density (19.68 tex), temperature and moisture conditions. By using a precision scale based on the ASTM standard D1907-01 [30], the linear densities of the thick and thin regions of each slub type were measured. Thick and thin places of the slub yarn were cut off and the length and weight measured. For each slub yarn, thirty tests were done for each thick and thin region, the results of which are indicated in ***Table 1***. The slub yarns have been coded 1 to 5. The regular sample has been denoted as No. 6.

A Zwick tester, made in Germany, model 1446-60, was used to perform tensile tests based on the ASTM standard D2256-02 [31]. In this part, tensile parameters of the slub yarn were measured, Where the gauge length was 500 mm and the rate of elongation was set at 50 mm/minute. In each case, 30 specimens were tested. The average results of the stress at the breaking point of yarns, $\sigma_{max(yarn)}$ are shown in ***Table 1***.

According to ***Table 1***, it can be seen that the highest slub count and the lowest base count belonged to sample number 2, showing poor tensile properties because it had a finer slub and base in comparison to other samples. Images of the uneven pattern could be seen better in sample number 2 due to the high difference between the base and slub count of this sample.

Production of fabrics

The sample yarns were used as weft to produce fabric using an F44 shuttle weaving machine. The warps, which consisted of cotton/polyester yarns, were the same for all fabric types. The linear density and thread density of the warps were 19.68 tex and 22 threads per centimeter, respectively. The density of the weft was set at 16 picks per centimeter.

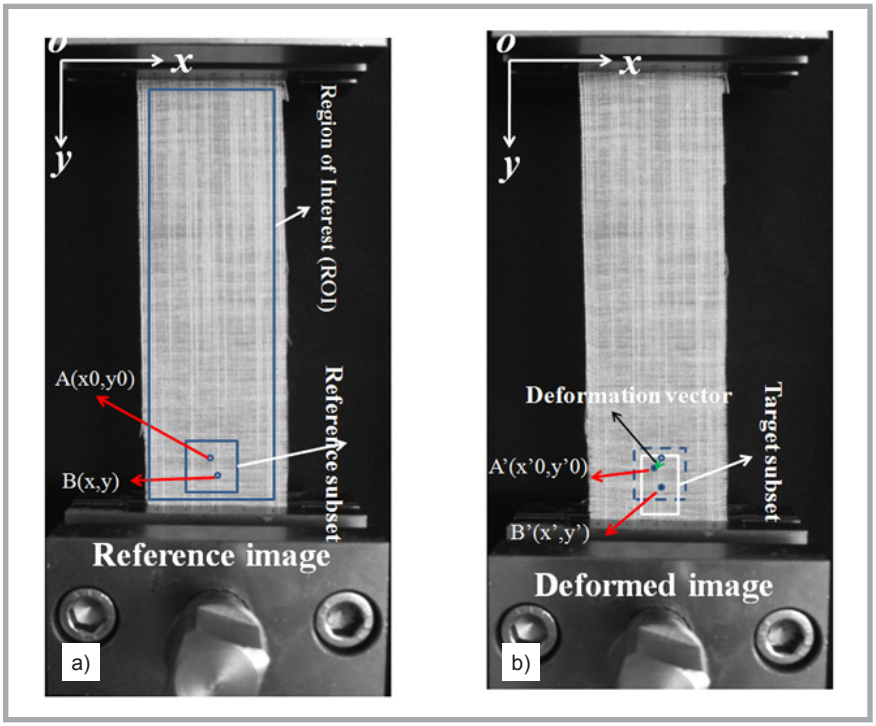

Figure 2. *Basic principles of the subset-based DIC method: a) tracking the same pixel point in the reference and b) getting a deformed image yielding its displacement vector.*

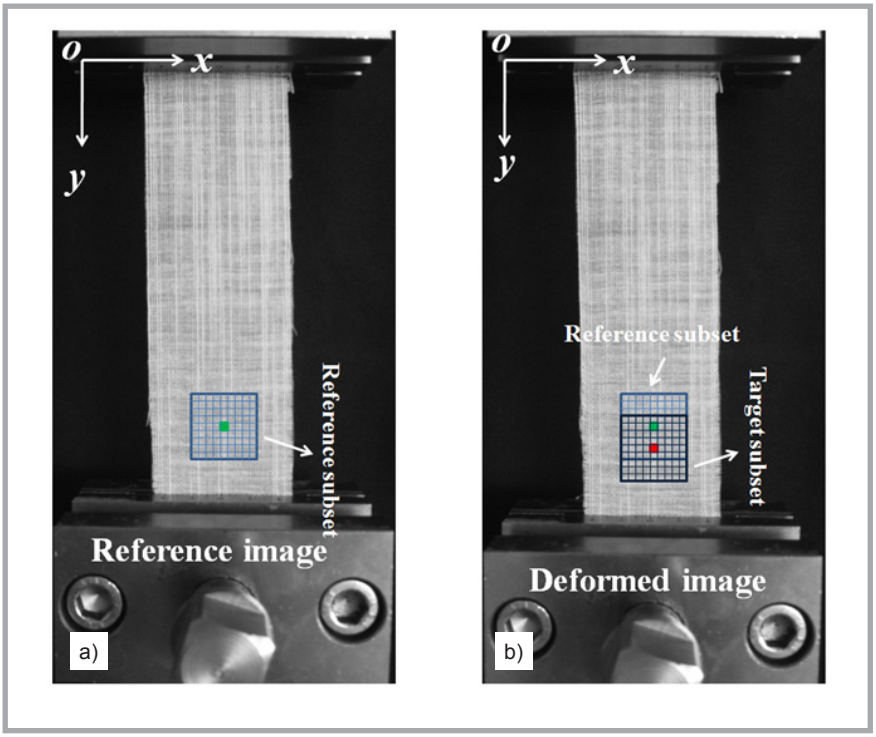

Figure 3. *Schematic view of a subset square size of 9 × 9 pixels in: a) the reference image and b) the reference and the deformed image together.*

Fabric testing

Tensile responses of the samples were tested using a uni-axial tensile testing machine (Zwick universal testing machine-144660) under the standard condition. To perform the tensile tests, samples of 50 × 250 mm were prepared based on ASTM standard D5035-95 [32]. The cut samples were fixed firmly to provide a gauge length of 150 mm with a sample width of 50 mm. The speed of the moving bottom jaw was set at 2 mm/minute. For each fabric sample, four specimens were tested. Results of the tensile property of the fabrics are shown in ***Table 2***.

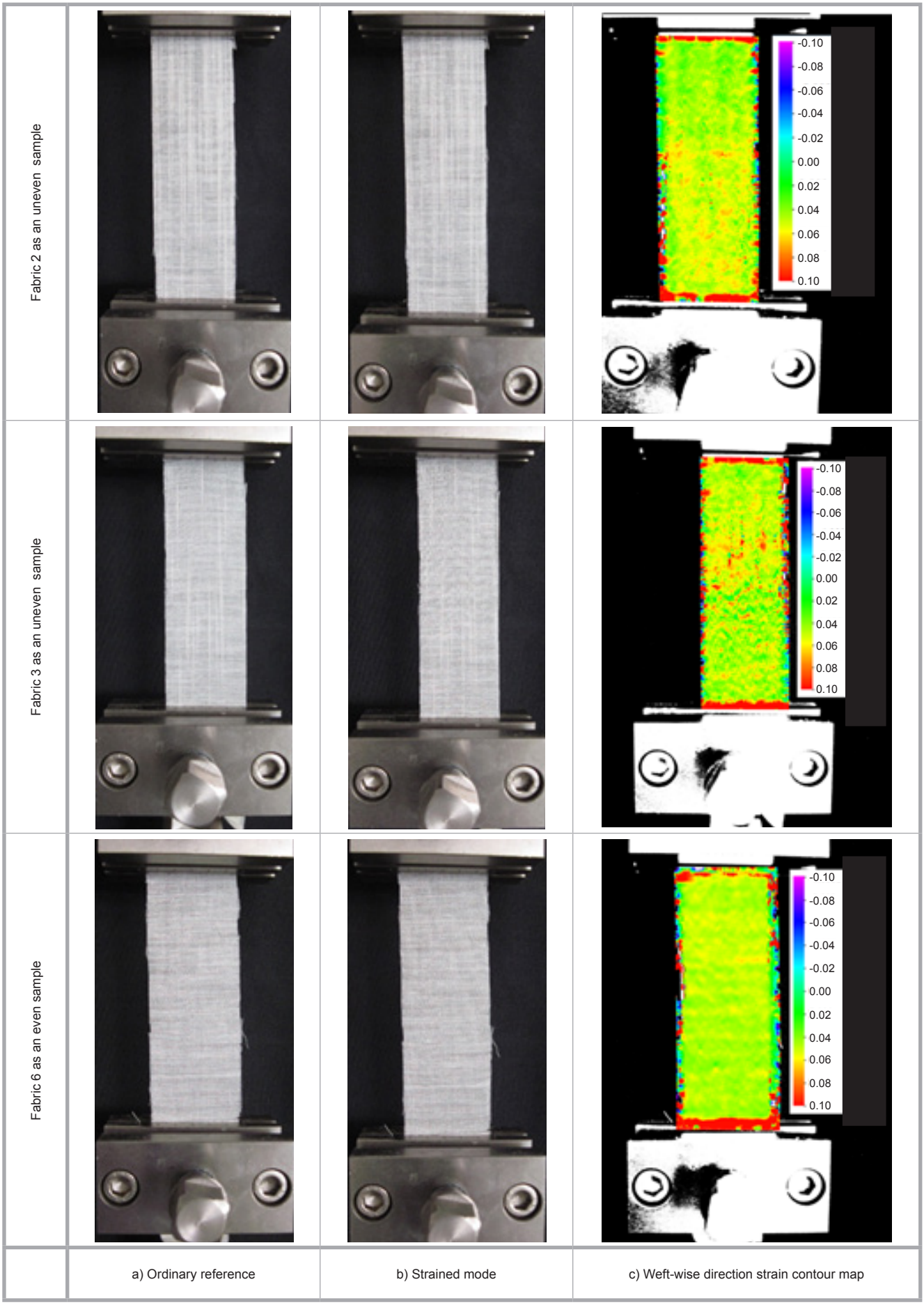

Figure 4. *Strain monitoring.*

The DIC method was used to investigate the strain field of the specimen throughout the test. To calculate the displacement field on the fabric surface, we used two sequent images based on the particle image and tracking velocimetry (PIV/PTV) technique. Photographs with a resolution of 12.1 million pixels were taken by CCD camera for every 2 mm crosshead displacement. For example, in a regular sample, we captured 8 photos up to the rupture point. The procedure was continued up to the rupture point of the fabric. Some photos of fabrics are shown in ***Figure 2*** (see page 75). The photos were processed by DIC software called Moire_0.950 [33]. A square reference subset is selected to track the same point (or pixel) and find its corresponding location in the target image. The size of this square subset was set to 21 × 21 pixels. The displacements and, finally, strains in each increment were calculated and visualised by contour maps on the input images.

Principles of standard subset-based digital image correlation

It is known that the non-contact DIC method is commonly employed for measuring full-field displacements in 2D and 3D. Based on this method, it is essential to first define a ROI (region of interest) in the reference image. Then this region is divided into evenly spaced virtual grids. Full-field deformation can be achieved by computing the displacement at the point of the virtual grids. ***Figure 2*** schematically shows the principle of the subset-based DIC. A square reference subset, which is centered at the current point $A(x0, y0)$ from the reference image, is selected to track the same point (or pixel) and find its corresponding location in the target image. The size of this square subset is known as (2M+1) × (2M+1) pixels, where M is the pixel number of the center point in the subset square. Displacement components of the reference and target subset centres can be obtained by finding the location of the target subset in the deformed image.

The displacement components of the same point in the reference and target images are then accurately estimated by digital image correlation on the basis of maximising the correlation coefficient. The Zero-mean Normalized Cross-Correlation (ZNCC) coefficient, as represented in ***Equation 1*** (see page 78), is employed for evaluation of the similarity of the reference and target subsets [34].

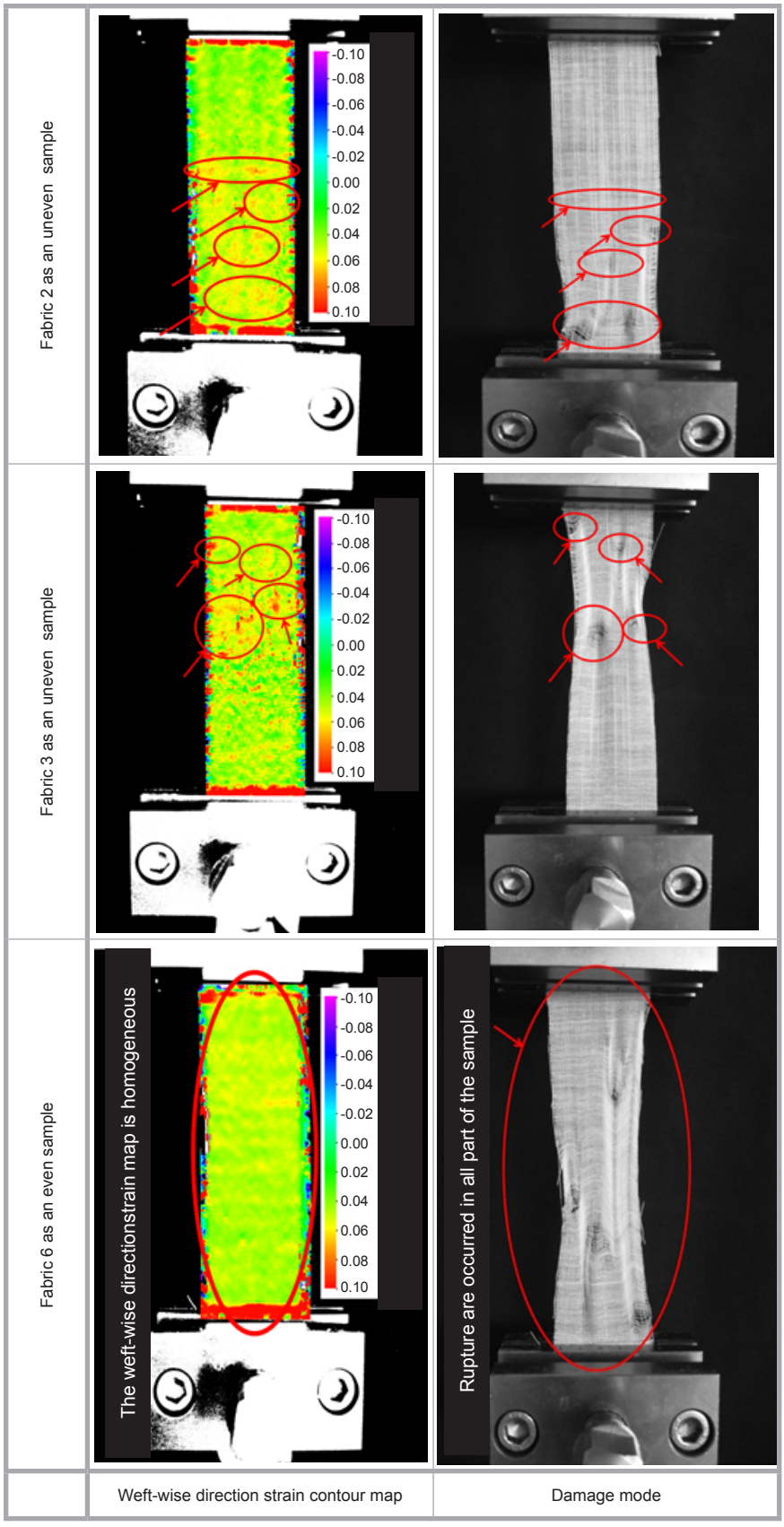

Figure 5. *Damage points prediction.*

It should be noted that the ZNCC coefficient is insensitive to the scale and the offset of illumination lighting fluctuations.

In ***Figure 1***, where, $f(x, y)$ is the gray level intensity at coordinates (x, y) in the reference subset of the reference image, while $g(x', y')$ is the gray level intensity

$$C_{ZNCC}(\mathbf{P}) = \frac{\sum_{x=-M}^{M}\sum_{y=-M}^{M}\left[f(x,y)-f_m\right]\times\left[g(x',y')-g_m\right]}{\sqrt{\sum_{x=-M}^{M}\sum_{y=-M}^{M}\left[f(x,y)-f_m\right]^2}\sqrt{\sum_{x=-M}^{M}\sum_{y=-M}^{M}\left[g(x',y')-g_m\right]^2}} \quad (1)$$

Equation 1

at coordinates (x', y') in the target subset of the deformed image. Also f_m and g_m, represent the mean intensity values of the reference and target subsets, respectively. **P** refers to the desired deformation vector [34].

The relationship between location (x, y) and (x', y') can be described as follows:

$$x' = x + u \quad (2)$$

$$y' = y + v \quad (3)$$

Where u and v represent the displacement of the pixel of (x, y) in the horizontal and vertical directions, respectively. One subset square size of 9 × 9 pixels in the reference image can be seen in ***Figure 3.a*** (see page 75) and the deformed image is schematically shown in ***Figure 3.b***. A green pixel stands for the subset square center in the reference image, while a red pixel represents the subset square centre in the deformed image.

Results and discussion

DIC results

DIC software, based on the procedure mentioned above, was used for determination of fabric samples' strain distribution and also prediction of the onset of rupture points. The output of the analysis could be in the form of the schematic or numeric mode. As mentioned before, a tensile test was performed in the weft direction; the direction in which the slub yarns were used. In other words, the wefts were aligned in the direction of the stress applied. In this work, the strain distribution in both the warp and weft directions of the fabric could be obtained. We studied only the strain in the weft direction, which was the direction of the stress applied.

Strain monitoring in fabric

The strain distribution was obtained by DIC software in the schematic and numerical mode. ***Figures 4.a*** and ***4.b*** (see page 76) show the ordinary reference (the first image with zero crosshead displacement) and a deformed mode of fabric (the fifth image with an 8mm crosshead displacement equal to 5.33 percent strain), respectively. ***Figure 4.c*** shows the weft-wise direction strain distribution in the colour-coding scheme with respect to the reference state. The sequence of the strain value in the colour-coding was from purple to red, corresponding to very low to very high strain, respectively.
It is necessary to mention that the small range of strain was selected to obtain a precise answer in the schematic ***Figure 4***.

As can be seen in ***Figure 4***, distributions of strain were more uneven in the case of slub yarns (samples 2 and 3). The concentration of strain was observed in the weft-wise direction of the strained fabric (points which are red or yellow). On the other hand, in sample 6, which was the regular sample, the distribution of strain was more even and smooth.

The strain distribution at the edge of the sample rectangle presented was not precise. The reason could be that the top and bottom margins were in contact with the tester jaws, and surely withstood further strain concentration. In the right and left margins, yarns were free and not engaged with others. It must be mentioned that in this study, the weft-wise direction strain was more important because slub yarns were aligned in the weft direction.

Damage prediction in the fabric surface

By applying this software, we can obtain the strain distribution in the damaged zone of the fabric. To do this, the software considered the reference image (***Figure 4.a***) and the strained fabric image (***Figure 4.b***) and provided a schematic image of the strained fabric (***Figure 4.c***). From the image of strain distribution in this stage, the critical regions could be marked. From this schematic image, the position of the damaged region in next stage could be predicted. ***Figure 5.b*** shows the actual image of the fabric in the damage mode. As can be seen, the damage zones were initiated in the regions, thereby showing high strain in ***Figure 5.a*** (see page 79).

As can be seen from ***Figure 5***, the strain distribution in the slub fabric (samples 2 and 3) was more irregular in comparison to the regular fabric (sample 6). In the regular sample, the strain distribution was more even,which means that the regular fabric was extended evenly in all fabric locations. In other words, it prevented stress concentration in a specific

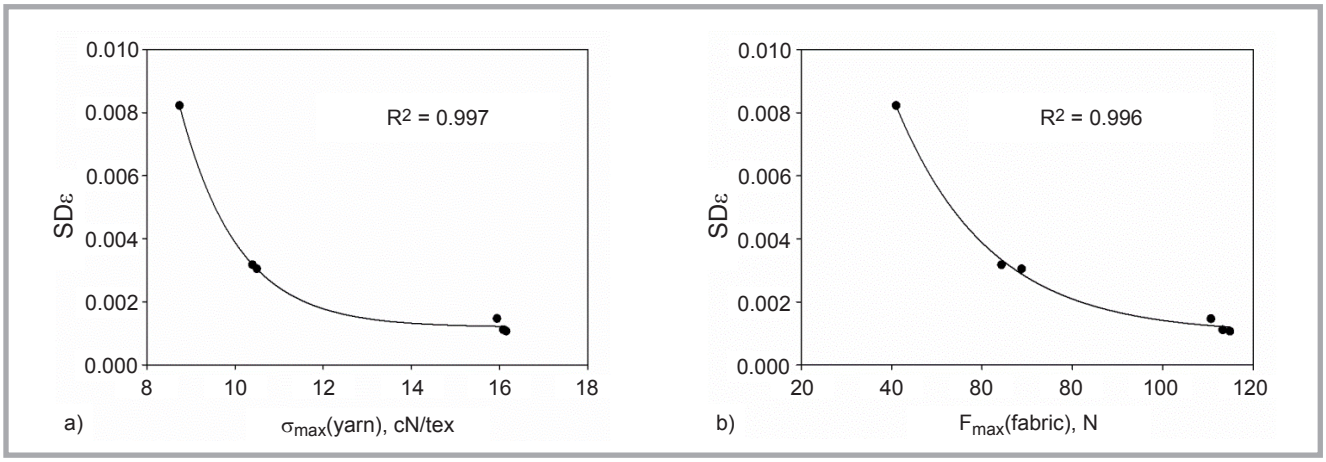

Figure 6. *The correlated plots of the SD_ε values versus; a) σ_{max} and b) F_{max}(fabric).*

Table 3. Variations of strain distribution in the fabrics.

Sample	1	2	3	4	5	6
SD_ε	0.00147	0.00823	0.00305	0.00112	0.00318	0.00107

location, and hence it was difficult to predict the damage region by DIC. The fabric was damaged randomly, as observed in ***Figure 5*** and sample 6.

Correlation between the strain distribution and slub yarn parameters

To investigate the variations in the strain distribution in the fabric, SD_ε was defined and calculated for the same rectangle selected by Moire 0.950 software. SD_ε was the standard error of the strains between all nodes in the strain map. The results are shown in ***Table 3***. No significant statistical correlations were observed between the variations in the strain distribution (SD_ε) and slub yarn parameters, as shown in ***Table 1***. In the next stage, we studied the correlation between the variation of the strain distribution (SDε) and the tensile properties of the yarn and fabric, as shown in ***Tables 1*** and ***2***.

Values plots of SD_ε versus σ_{max} and F_{max}(fabric) are shown in ***Figures 6.a*** and ***6.b***, respectively. In these figures, the vertical axis represents SD_ε values and the horizontal axis stands for σ_{max} and F_{max}(fabric) values. According to ***Equations 4*** and ***5***, the data points were in acceptable exponential correlations with a correlation coefficients (R-square) of 0.997 and 0.996 [35].

$$SD_\varepsilon = 0.0012 + 5.5693\exp(-0.7636 \times F_{max}) \quad (4)$$

$$SD_\varepsilon = 0.001 + 0.0524\exp(-0.0483 \times \sigma_{max}) \quad (5)$$

It can be observed in the plots of ***Figure 6*** that the variation in the strain distribution in the elements of the stretched fabric followed an exponential trend and was inversely related to the breaking tenacity of the yarn as well as the breaking strength of the fabric. With an increase in the breaking tenacity of the yarn, the variations in the strain distribution in the fabric decreased sharply, meaning that increasing yarn breaking tenacity led to a more even distribution of strain in the fabric during the tensile test. As the tenacity of the yarn was increased to a higher level, the variations in the strain distribution reached a constant level. In other words, after a certain tenacity, the increase in yarn tenacity had no significant effect on the strain distribution. The same explanation can be employed for the effect of fabric failure strength on the strain distribution during the tensile test.

Conclusions

In this work, the effect of locally induced mass irregularities of weft yarn on the strain distribution of fabric during a tensile test was investigated. Five different types of slub yarns plus a regular yarn were produced. The yarns were then used as the weft in a plain-woven fabric. A tensile test was perfumed on the fabric. The DIC method was also employed to evaluate the strain distribution of the fabric during the tensile test. An image of the reference samples and deformed fabric near the damage region was considered and the strain distribution map of the fabric was calculated. The results were compared with an image of the actual fabric at the same stage, near the damage mode.

The main conclusions of this study are:

- Slub yarn parameters such as slub length and slub distance affect the irregularity of yarn. This, in turn, leads to local irregularity of the fabric surface. The results show that the procedure is an acceptable method to identify and predict the strain distribution of the fabric and its actual strain concentration during the tensile test (strain distribution variation value and strain distribution contour map).
- The results also revealed that the DIC method could be used to predict the damage regions of the fabric during the tensile test.
- It was also shown that there was an exponential correlation between the strain variation in the fabric elements during the tensile test and the tenacity in cN/tex of the yarns produced, with a regression coefficient (R-square) greater than 0.99.
- A small increase in the breaking tenacity in cN/tex of slub yarns leads to a large reduction in strain variation in the fabric elements because of the exponential relation between them.
- There was an exponential correlation between the strain variation in the fabric elements during the tensile test and breaking strength in N of the fabric, with a regression coefficient (R^2) greater than 0.99.
- A small increase in the breaking strength in N of the fabric leads to a large reduction in strain variation in the fabric elements because of the exponential relation between them.

References

1. Grabowska KE and Ciesielska-Wróbel I. Characteristic and Application of Knop Fancy Yarns. *Fibres & Textiles in Eastern Europe* 2015; 23, 1(109): 17-25.
2. Grabowska KE. Comparative Analysis of Fancy Yarns Produced on a Ring Twisting System. *Fibres & Textiles in Eastern Europe* 2010; 18, 1(78): 36-40.
3. Ilhan I, Babaarslan O and Vuruskan D. Effect of Descriptive Parameters of Slub Yarn on Strength and Elongation Properties. *Fibres and Textiles in Eastern Europe* 2012; 20, 3(92): 33-38.
4. Lu Y, Gao W and Wang H. A model for the twist distribution in the slub-yarn. *International Journal of Clothing Science and Technology* 2007; 19: 36-42.
5. Ilhan I, Babaarslan O and Vuruskan D. A Theoretical Model and Practical Observation for Prediction of Slub Yarn Counts. *TekstilvaKonfeksiyon* 2010; 20: 306-312.
6. Souid H, Babay A, Sahnoun M and Cheikrouhou M.. A Comparative Quality Optimization Between Ring Spun and Slub Yarns By Using Desirability Function. *AUTEX Research Journal* 2008; 8:72-76.
7. Pan R, Gao W, Liu J and Wang H. Recognition the Parameters of Slub-yarn Based on Image Analysis. *Journal of Engineered Fibers and Fabrics* 2011; 6: 25-30.
8. Moezzi M, Ghane M, Nicoletto G and JafariNedoushan R.. Analysis of the mechanical response of a woven polymeric fabric with locally induced damage. *Material & Design* 2014; 54: 79-90.
9. Lijun Q, Zhang Z, Li X, Yang X, Feng Z, Wang Y, Miao H, He L and Gong X.. Full-field analysis of shear test on 3D orthogonal woven C/C composites. *Composites*: *Part A: Applied Science and Manufacturing* 2012; 43: 10-16.
10. Ragaiiene A and Milaiene D. Mathematical Simulation of Elongation at Break after Fatigue Loading of Fabrics Containing Fancy Yarns. *Fibres & Textiles in Eastern Europe* 2013; 21, 4(100): 67-74.
11. Devivier C, Pierron F, and Wisnom MR. Damage detection in composite materi-

Institute of Textile Engineering and Polymer Materials

The Institute of Textile Engineering and Polymer Materials is part of the Faculty of Materials and Environmental Sciences at the University of Bielsko-Biala. The major task of the institute is to conduct research and development in the field of fibers, textiles and polymer composites with regard to manufacturing, modification, characterisation and processing.

The Institute of Textile Engineering and Polymer Materials has a variety of instrumentation necessary for research, development and testing in the textile and fibre field, with the expertise in the following scientific methods:

- FTIR (including mapping),
- Wide Angle X-Ray Scattering,
- Small Angle X-Ray Scattering,
- SEM (Scanning Electron Microscopy),
- Thermal Analysis (DSC, TGA)

Strong impact on research and development on geotextiles and geosynthetics make the Institute Institute of Textile Engineering and Polymer Materials unique among the other textile institutions in Poland.

Contact:
Institute of Textile Engineering and Polymer Materials
University of Bielsko-Biala
Willowa 2, 43-309 Bielsko-Biala, POLAND
+48 33 8279114,
e-mail: itimp@ath.bielsko.pl
www.itimp.ath.bielsko.pl

als using deflectometry, a full-field slope measurement technique. *Composites: Part A: Applied Science and Manufacturing* 2012; 43: 50-66.
12. Caminero MA, Lopez-Pedrosa M, Pinna C and Soutis C. Damage monitoring and analysis of composite laminates with an open hole and adhesively bonded repairs using digital image correlation. *Composites: Part B: Engineering* 2013; 53: 76-91.
13. Xin B and Hu J. An image based method for characterizing the mechanical behaviors of fabrics. Part 1: The measurement of in-plane tensile behavior. *Fibres and Textiles in Eastern Europe* 2008; 16, 1(66): 72-75.
14. Xin B, Li Y, Qiu J and Liu Y. Texture modeling of fabric appearance evaluation based on image analysis. *Fibres and Textiles in Eastern Europe* 2012; 20, 2(91): 48-52.
15. Ezazshahabi N, Latifi M and Madanipour K.. Surface roughness assessment of woven fabrics using fringe projection moiré techniques. *Fibres and Textiles in Eastern Europe* 2015; 23, 3(111):76-84.
16. YekaniFard M, Sadat SM, Raji BB and Chattopadhyay A. Damage characterization of surface and sub-surface defects in stitch-bonded biaxial carbon/epoxy composites. *Composites: Part B: Engineering* 2014; 56: 821-829.
17. Chu TC, Ranson WF, Sutton MA, and Peters WH. Applications of digital-image-correlation techniques to experimental mechanics. *Experimental Mechanics* 1985; 25: 232-244.
18. Pan B, QianK M, Xie HM and Asundi A.. Two-dimensional Digital Image Correlation for In-plane Displacement and Strain Measurement: A Review. *Measurement Science and Technology* 2009; 20: 062001.
19. Pan B, Xie HM, Xu BQ and Dai FL. Performance of sub-pixel registration algorithms in digital image correlation. *Measurement Science and Technology* 2006; 17: 1615-1621.
20. Pan B, Asundi A, Xie H M and Gao J X. Digital Image correlation using iterative least squares and point wise least squares for displacement field and strain field measurements. *Optics and Lasers in Engineering* 2009; 47: 865-874.
21. Jin H Q and Bruck H A. Theoretical development for pointwise digital image correlation. *Optical Engineering* 2005; 44: 1-14.
22. Cheng P, Sutton MA, Schreier HW and McNeill SR. Full-field speckle pattern image correlation with B-spline deformation function. *Experimental Mechanics* 2002; 42: 344-352.
23. Sun Y, Pang JHL, Wong CK and Su F. Finite element formulation for a digital image correlation method. *Applied Optics* 2005; 44: 7357-7363.
24. Besnard G, Hild F and Roux S. Finite-element displacement fields analysis from digital images: application to Portevin-le chaterlier bands, *Experimental Mechanics* 2006; 46: 789-803.
25. Rethore J, Hild F and Roux S. Shear-band capturing using a multiscale extended digital image correlation technique. *Computer Methods Applied Mechanics Engineering* 2007; 196: 5016-5030.
26. Rethore J, Hild F and Roux S. Extended digital image correlation with crack shape optimization. *International journal of Numerical Methods in Engineering* 2008; 732: 248-272.
27. Bruck HA, McNeil SR, Sutton MA and Peters WH. Digital image correlation using Newton-Raphson method of partial differential correction, *Experimental Mechanics* 1989; 29: 261-267.
28. Vendroux G and Knauss WG. Submicron Deformation Field Measurements: Part 2 improved Digital Image Correlation. *Experimental Mechanics* 1998; 38: 86-92.
29. Pan B. Reliability-guided digital image correlation for image deformation measurement. *Applied Optics* 2009; 48: 1535-1542.
30. ASTM International. (2001).*Standard Test Method for Linear Density of Yarn (Yarn Number) by the Skein Method*, ASTM D 1907- 01. West Conshohocken, PA: Annual book of ASTM standards.
31. ASTM International. (2002). *Standard Test Method for Tensile Properties of Yarns by the Single-Strand Method1*, ASTM D 2256- 02. West Conshohocken, PA: Annual book of ASTM standards.
32 ASTM International (1995) *Standard test method for breaking force and elongation of textile fabrics (strip method)*, ASTM D 5035- 95. West Conshohocken, PA: Annual book of ASTM standards.
33. http://www.opticist.org/node/73.
34. Pan B, Xie HM, Guo ZQ and Hua T. Full-field strain measurement using a two-dimensional Savitzky-Golay digital differentiator in digital image correlation. *Optical Engineering* 2007; 46: 033601.
35. Montogomery DC. *Introduction of Linear Regression Analysis*, 5th ed. meas Hoboken, New Jersey: Wiley Series in Probability and Statistics, 2012.

Received 15.07.2015 Reviewed 27.09.2015